

Photothermal and Conductive Composite Hydrogel Membrane for Solar-Driven Synchronous Desalination and Salinity Power Generation

Hongjiang He,^a Xi-Ming Song,^a Mengnan Huang,^c Xing Hou,^a Zhining Song^{*a} and Yu Zhang^{*a, b}

^a *Liaoning Key Lab for Green Synthesis and Preparative Chemistry of Advanced Materials, College of Chemistry, Liaoning University, Shenyang 110036, China*

^b *Hangzhou Xigu Technology Co., Ltd. Hangzhou 310000, China.*

^c *Key Lab of Rare-scattered Elements of Liaoning Province, College of Chemistry, Liaoning University, Shenyang 110036, China*

**Corresponding authors. E-mail:*

songzhining@lnu.edu.cn (Zhining Song); zhangy@lnu.edu.cn (Yu Zhang)

1. Experimental section

Materials

Carbon black, carbon nanotubes purchased from the company. Sodium alginate and calcium chloride were purchased from Sino-pharm Chemical Reagent Company Limited. Nickel foam was purchased from OPV Tech New Energy Company Limited. Graphene oxide (GO) and polypyrrole (PPY) were synthesized by previously reported methods.^{1,2}

Preparation of hybrid power system

Firstly, sodium alginate (2 g) and deionized water (98 mL) were added in a glass beaker and stirred continuously for 12 h at 60 °C. Subsequently, carbon black (0.1 g) was added in sodium alginate aqueous solution (6 mL) and stirred continuously for 1 h to obtain a homogeneous alginate aqueous solution. The mixture was coated on the nickel foam under 10 MPa. A polyethylene foam (5.5 cm diameter, 0.5 mm thickness) was laminated on the nickel foam. Polyethylene foam was used as a floating evaporation structure to make the hybrid power system float on the water, and 5 round holes with 6 mm diameter were evenly cut out, in which sodium alginate solution was filled to supply water to the photothermal layer at the top. Finally, the multiple-layer structure was immersed in calcium chloride solution (40 mL, 0.05 g mL⁻¹) for 60 min, and the glass plate was stripped to obtain CHN-CB. The preparation of hybrid power systems based on other photothermal materials is similar.

Solar energy interface evaporation test

During the solar evaporation test, the hydrogel membranes on the loaded water were irradiated at room temperature (25 °C) with a xenon lamp as a solar simulator. Changes in the temperature of the sample surface and water were monitored by an infrared thermal imager. The amount of water loss was recorded using an electronic balance.

Electrochemical characterization

The current-voltage curves and photocurrent density-time (i-t) were tested in a two-electrode system including the CHNs as the working electrode and Pt/O₂ as the counter electrode.

Materials Characterization

The morphology of the sample was observed by using a scanning electron microscope (SEM, Hitachi SU8010). UV-vis spectroscopy and diffuse reflectance spectroscopy (DRS) were tested on a UV-vis spectrometer (Shimadzu UV-2600) by using the semiconductor films. Differential scanning calorimetric (DSC) measurements were performed on differential scanning calorimetry (DSC8500, PerkinElmer). The ion concentration inside the hydrogel was tested by an ion chromatograph (ICS-900, Dionex, America). The internal potential test of hydrogel is to ultrasonic milled hydrogel for 3h, filter it with a molecular sieve with pore size of 500 nm, and then perform zeta potential test (ZEN1002). During the solar evaporation test, the hydrogel film was irradiated at room temperature (25 °C) with a xenon lamp as a solar simulator. Changes in the temperature of the sample surface and water were monitored by an infrared thermal imager. The amount of water loss was recorded using an electronic balance. The electrical measurements were conducted with an electrochemical workstation (CHI660E, Shanghai). The current-voltage curves of the hybrid device were performed at a scan rate of 100 mV s⁻¹.

2. Supplementary Notes

Note 1. Solar evaporation efficiency

Solar evaporation efficiency is calculated as: ³

$$\eta = \dot{m}h_v / C_{opt}P_o \quad (1)$$

Where \dot{m} is the mass flux, h_v is the enthalpy of vaporization of water in the greenhouse, P_o is the solar irradiation power of 0.5 sun (0.5 kW m⁻²), and C_{opt} is the optical concentration of the absorber surface.

Note 2. Salinity power⁴

According to the previous works, in the NaCl electrolyte:

$$E_{redox} = \frac{RT}{F} \ln \left(\frac{c_H \gamma_H}{c_L \gamma_L} \right) \quad (2)$$

Because $t_+ + t_- = 1$,

$$E_{diff} = (t_+ - t_-) \frac{RT}{F} \ln \left(\frac{c_H \gamma_H}{c_L \gamma_L} \right) = (2t_+ - 1) \frac{RT}{F} \ln \left(\frac{c_H \gamma_H}{c_L \gamma_L} \right) \quad (3)$$

where t_+ , t_- , R , T , F , γ , c_H , and c_L represent the transference number of cations and anions, gas constant, temperature, Faraday constant, activity coefficient of ions, high and low ion concentrations, respectively. The voltage detected by electrochemical workstation is the sum of E_{redox} and E_{diff} , which can be expressed as:

$$E = E_{diff} + E_{redox} = 2t_+ \frac{RT}{F} \ln \left(\frac{c_H \gamma_H}{c_L \gamma_L} \right) \quad (4)$$

Note 3. Energy efficiency analysis

The free energy change from mixing two different concentrations of solution can be written as:

$$\Delta G = 2RTV_H \left[c_H \ln \frac{c_H(1+\varphi)}{c_H + \varphi c_L} + \varphi c_L \ln \frac{c_L(1+\varphi)}{c_H + \varphi c_L} \right] \quad (5)$$

where ΔG is the free energy (J), V the volume (m^3), and $\varphi = V_L/V_H$. H refers to the high concentration solution and L to the low concentration solution. When the hybrid device arrives to steady-state under solar irradiation, steam generates on the light absorber with a rate of v ($m^3 (m^{-2} s^{-1})$), the theoretical power density of the formed salinity P ($W m^{-2}$) can be expressed as:

$$P = \frac{\Delta G v}{V_H} \quad (6)$$

When φ is large enough, the value of ΔG will reach to a limiting value for a certain V_H .

3. Supplementary Figures

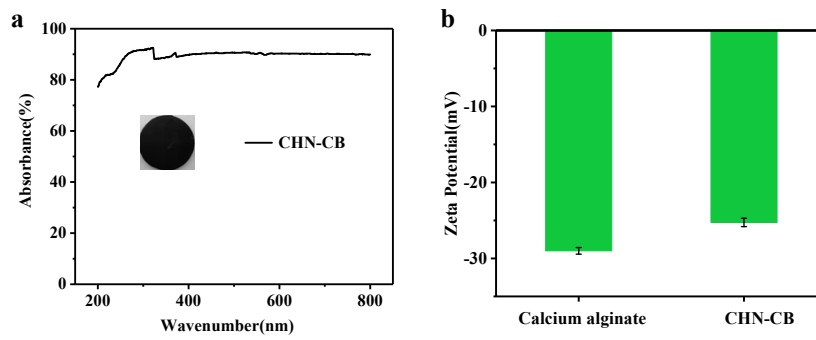


Figure S1 Characterization of CHN-CB membrane. (a) Adsorption spectrum of CHN-CB membrane. The illustration is the photograph of CHN-CB. (b) Internal potential of calcium alginate and CHN-CB.

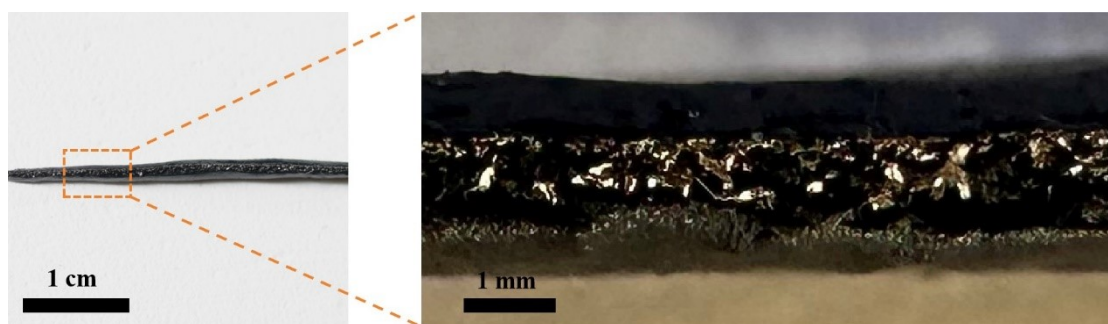


Figure S2 The photograph of cross-section of the CHN-CB membrane.

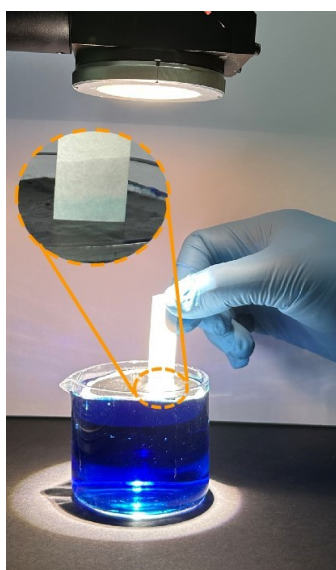


Figure S3 The hydrophilicity test of the CHN-CB membrane. The stain was found on the upper surface of the CHN-CB membrane after evaporation for 13 min under 1 sun when the water stained with methylene blue was used for the evaporation experiment, indicating the flux of water and the hydrophilicity of the CHN-CB membrane.

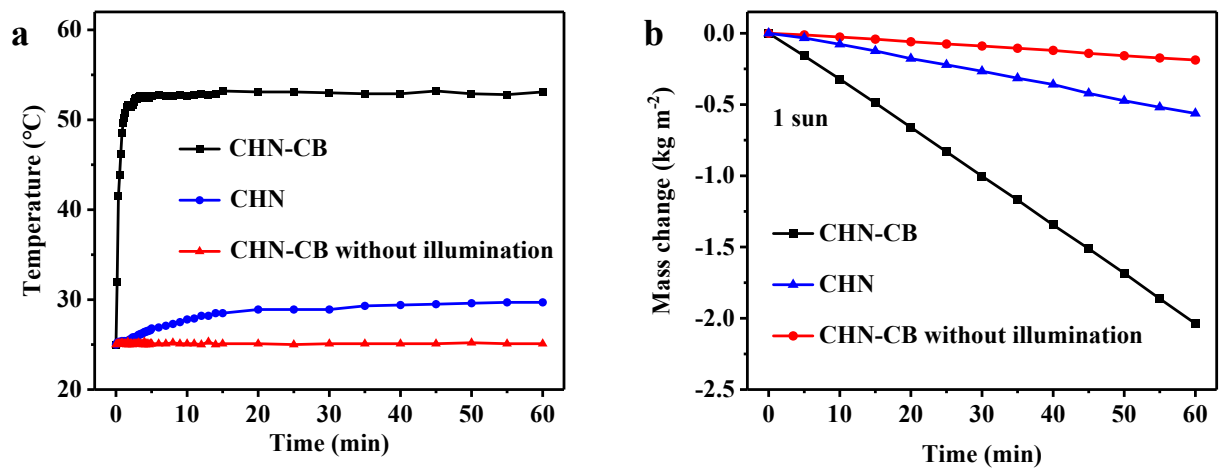


Figure S4 Under 1 sun (1 kW m^{-2}), (a) The surface temperature curve of CHNs. (b) The evaporation induced mass loss of water.

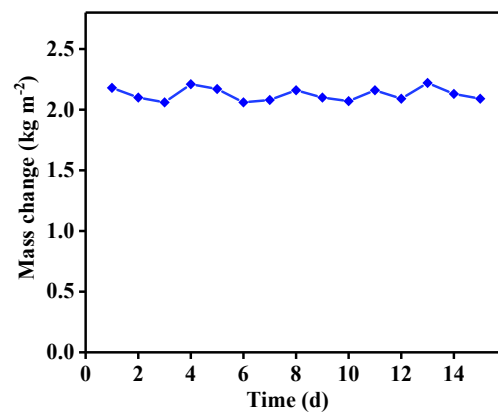


Figure S5 The evaporation rate of the CHN-CB membrane for 15 days.

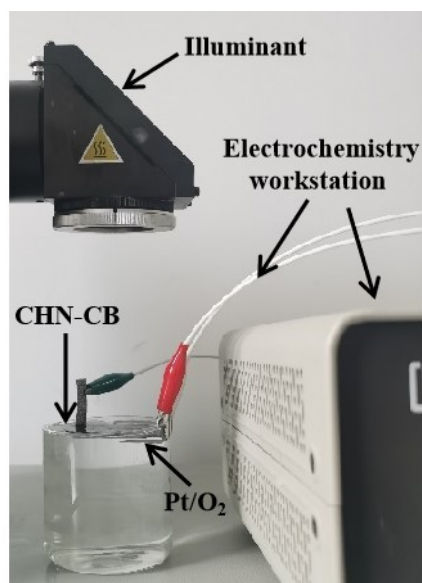


Figure S6 The evaporation-driven salinity power generation devices.

Table S1 The cost accounting of the evaporator.

Materials	unit price	dosage	expenditure	remark
SA	\$ 23.42/500 g	25.46 g/m ²	\$ 1.19	_____
CaCl₂	\$ 3.01/500 g	1018.33 g/ m ²	\$ 6.13	_____
nickel foam	\$ 74.89/m ²	1.00 m ²	\$ 74.89	reuse
carbon black	\$ 13.89/100 g	15.28 g/ m ²	\$ 2.12	_____
polyethylene foam	\$ 0.75/m ²	1.00 m ²	\$ 0.75	reuse
rest	_____	_____	\$ 0.05	_____
aggregate			\$ 85.13	

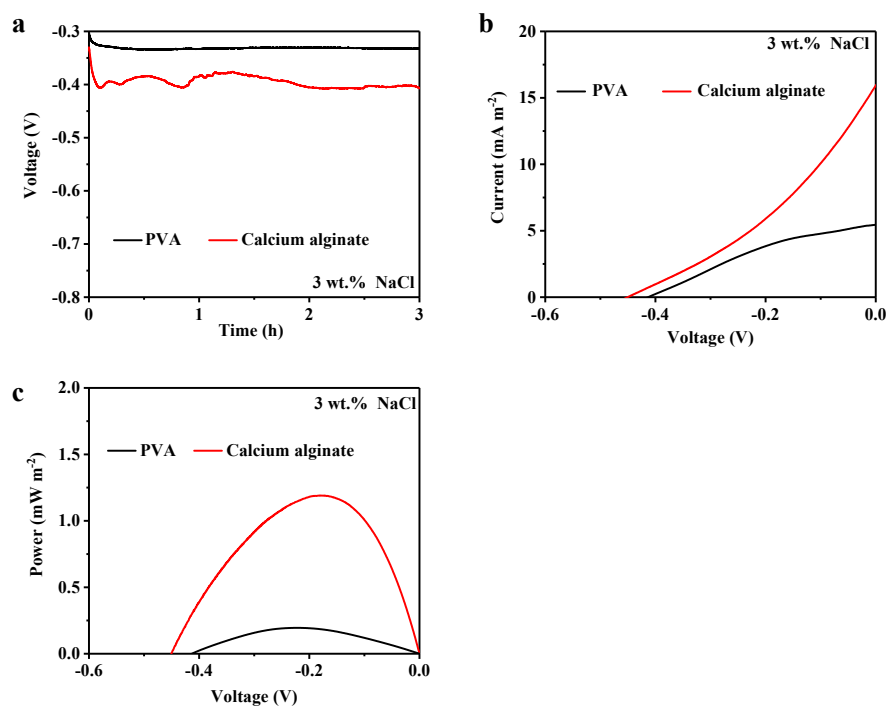


Figure S7 (a) The open-circuit voltage, (b) current-voltage curves, and (c) maximum output power of solar evaporators with different hydrogel compositions under illumination.

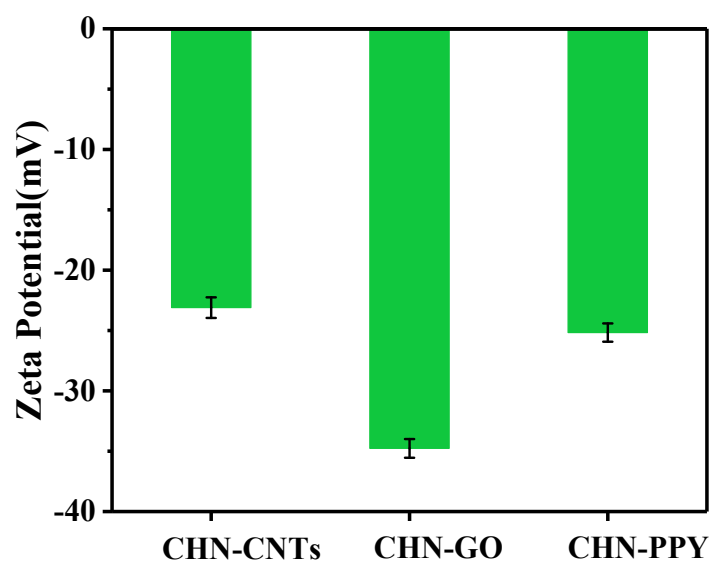


Figure S8 Internal potential of CHN-CNTs, CHN-GO, CHN-PPY membranes.

References

1. L. Liang, G. Chen and C.-Y. Guo, *Mater. Chem. Front.*, 2017, **1**, 380-386.
2. A. Dimiev, D. V. Kosynkin, L. B. Alemany, P. Chaguine and J. M. Tour, *J. Am. Chem. Soc.*, 2012, **134**, 2815-2822.
3. F. Zhao, X. Zhou, Y. Shi, X. Qian, M. Alexander, X. Zhao, S. Mendez, R. Yang, L. Qu and G. Yu, *Nat. Nanotechnol.*, 2018, **13**, 489-495.
4. P. Yang, K. Liu, Q. Chen, J. Li, J. Duan, G. Xue, Z. Xu, W. Xie and J. Zhou, *Energy Environ. Sci.*, 2017, **10**, 1923-1927.